JOURNAL OF MATERIALS SCIENCE **34** (1999) 5771–5776

Effects of particle size on thermal durability and microporous characteristics for sintered bodies of alumina-pillared fluorine micas

T. YAMAGUCHI*, Y. SAKAI, K. KITAJIMA
Department of Chemistry and Material Engineering, Faculty of Engineering, Shinshu University, Wakasato, Nagano 380-8553, Japan
E-mail: mtmouth@gipwc.shinshu-u.ac.jp

Powder compacts of alumina-pillared fluorine micas having different particle sizes were fired at various temperatures in the range of 500–800 °C. Sintered bodies of the alumina-pillared micas were obtained at 500–700 °C with retaining their pillared structure. The pillared structure collapsed at 800 °C, losing microporous characters. Specific surface area and micropore volume of the sintered bodies obtained from coarse particles are larger than those obtained from fine particles. Thermal durability of the pillared structure depends on the particle size of alumina-pillared fluorine micas, especially on the c*-dimension of the host mica crystals; thermal durability of the sintered bodies obtained from coarse particles is higher than that from fine particles. The sintered bodies are machinable due to the interlocking microstructure of the flaky mica crystals.

1. Introduction

The intercalation of bulky inorganic polycations into the interlayer region of swelling clay minerals followed by calcination allows the preparation of thermally stable microporous solids, i.e., pillared clays. In pillared clays, the intercalated oxides formed after calcination prop the layers apart as pillars. Pillared clays exhibit interesting properties for catalysis, adsorption and separation.

The present authors have focused their attention on expandable synthetic fluorine micas [1, 2] as host crystals for intercalation. These synthetic micas are featured by large cation exchange capacity and high crystallinity. The variability of layer charge also leads to the controlled pillar density and microporous properties for alumina-pillared [3], chromia-pillared [4], and titania-pillared [5] fluorine micas. Furthermore, reduction of 3d transition-metal ions into zero-valence metal was undertaken in the interlayer regions of cation exchanged fluorine micas [6].

In order to be more useful, pillared clays must be formed to a specific shape with controlled tolerances and known properties. The sintered bodies of pillared fluorine micas are expected to be obtainable without adding binders because fluorine mica complexes are expected to have sinterability at low temperatures due to their high chemical activity. The addition of binders in forming processes inevitably reduces microporous characters. Therefore, the sintered bodies of pillared fluorine micas having microporous characteristics will extend the use of pillared micas, however, sintering of pillared fluorine micas have not been reported. The control of microporous characters of sintered bodies is very important for their applications.

In this study, Na-Tetrasilicic fluorine mica, [$NaMg_{2.5}Si_4O_{10}F_2$] [1, 7], was used as the host crystals. The aims of this paper are (i) to obtain the sintered bodies of alumina-pillared fluorine micas without adding binders, (ii) to clarify the effect of the particle size of host crystals on thermal durability of the pillared structure, and (iii) to examine microporous characteristics of the sintered bodies. In consequence, we have succeeded in preparing the sintered bodies of alumina-pillared fluorine micas having high surface area and micropore volume.

2. Experimental

The starting Na-Tetrasilicic fluorine mica (hereafter denoted by Na-TSM), $NaMg_{2.5}Si_4O_{10}F_2$, was synthesized by the same procedure as described previously [1]. The crystals thus obtained were dispersed into distilled water and then classified by sedimentation to obtain the two groups of different particle sizes (hereafter denoted by coarse particles and fine particles). Hydroxoaluminum solution used as a pillaring agent was prepared by dissolving aluminum metal in HCl [8–10]. The solution had a OH/Al ratio of 2.495 and Al_2O_3 concentration of 23.2 wt %. Classified Na-TSM was allowed to react with the hydoroxoaluminum solution at 25 °C for 2 h under vigorous stirring. The reaction products were centrifuged, followed by washing with distilled water sufficiently and then dried in air at 60 °C. The amounts of intercalated Al were measured

* Author to whom all correspondence should be addressed.

by a gravimetric analysis after the mica samples were fused with Na_2CO_3. The powder samples were uniaxially compressed in vacuum at 300 MPa into disk compacts ($1.6 \times 13\phi$ mm). The compacts were heated in an electric furnace in the temperature range of 500–800 °C for 3 h in order to obtain fired samples. The changes in the dimension and weight with firing were measured for the compacts. Fractured surfaces of fired samples were observed using a scanning electron microscope (SEM). The fired samples were then crushed into powders in an agate mortar and basal spacings of pillared micas were measured by X-ray powder diffraction (XRD) (monochrometer with CuK_α). Coherent domains of crystallites were also measured from the (0 0 4) basal reflection by the line broadening method. Specific surface areas, pore size distributions and micropore volumes of the samples were calculated from adsorption-desorption isotherms for nitrogen at liquid nitrogen temperature. In addition, some fired bodies were subjected to boring tests using a drill with a diameter of 1.0 mm for the evaluation of machinability. The bending strength was also measured for fired bodies.

3. Results and discussion

Fig. 1 shows the SEM photographs of alumina-pillared fluorine mica crystals having different particle sizes. The flaky crystals of coarse particles were thicker than those of fine particles, showing a lower aspect ratio. For alumina-pillared micas obtained from both coarse particles and fine particles, the maximum dimensions parallel to the layers were about 10 μm and there were not so quite differences in the maximum lateral size each other. However, the coherent dimension perpendicular to the layers of host mica crystals was estimated to be 15 nm for fine particles and 50 nm for coarse particles from the line broadening of the (0 0 4) profile.

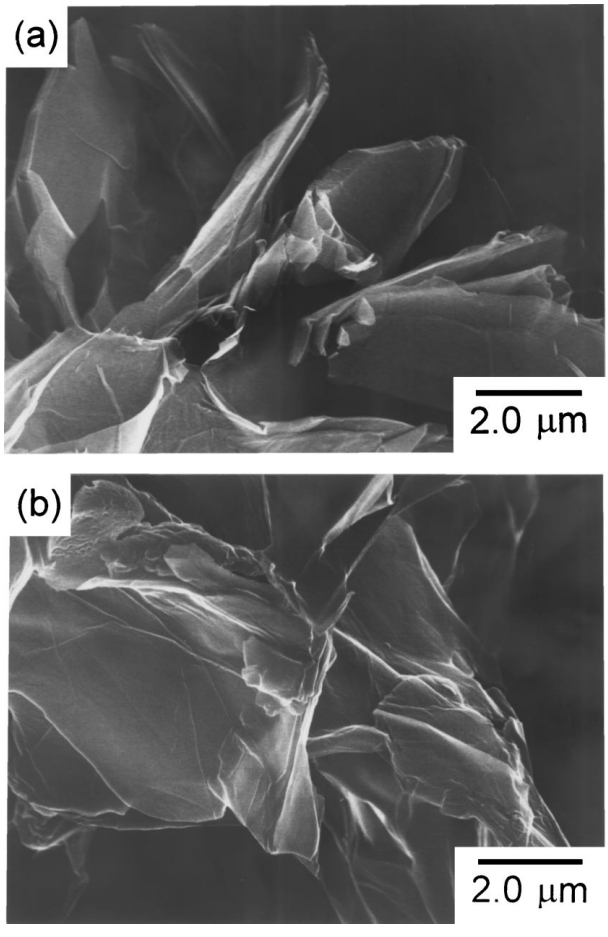

Figure 1 SEM photographs of alumina-pillared fluorine mica crystals having different particle sizes. (a) coarse particles, (b) fine particles.

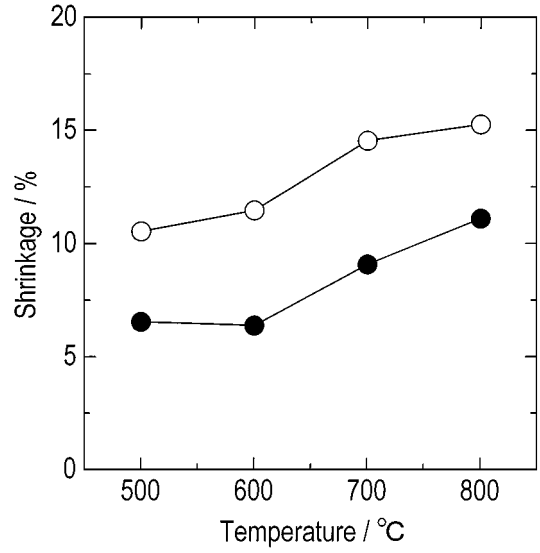

Figure 2 Shrinkage plotted against firing temperature for the sintered bodies of alumina-pillared fluorine micas having different particle sizes. ●: sintered body obtained from coarse particles, ○: sintered body obtained from fine particles.

On firing in the temperature range of 500–800 °C, sintered bodies showed no deformation and cracking. Fig. 2 shows the shrinkage of sintered bodies plotted against firing temperature for alumina-pillared fluorine micas having different particle sizes. The data of the shrinkage are shown only for the direction perpendicular to the disk compact plane. The standard deviation of the shrinkage was estimated to be 0.6%. The sintered bodies obtained from fine particles have larger shrinkage than those obtained from coarse particles. Although maximum lateral sizes of fine and coarse particles are similar, fine particles provide more densified and curled microstructure of interlocking platelets than coarse particles because fine particles are easily deformed upon heating due to their better flexibility based on their higher aspect ratios. The coarse particles having lower aspect ratios hinder densification due to their rigidity. The shrinkage increases with increasing firing temperature, indicating changes in porosity.

An anisotropic shrinkage between the directions parallel and perpendicular to the disk compact plane was observed. The shrinkage for the direction parallel to the disk plane was 16–24% of the shrinkage perpendicular to the plane. This is probably because the flakes of pillared micas tend to orient vertically to the pressing axis on molding.

Fig. 3 shows the bulk density of sintered bodies plotted against firing temperature. The standard deviation of the bulk density was estimated to be 0.02 g cm^{-3}. The sintered bodies obtained from fine particles have larger

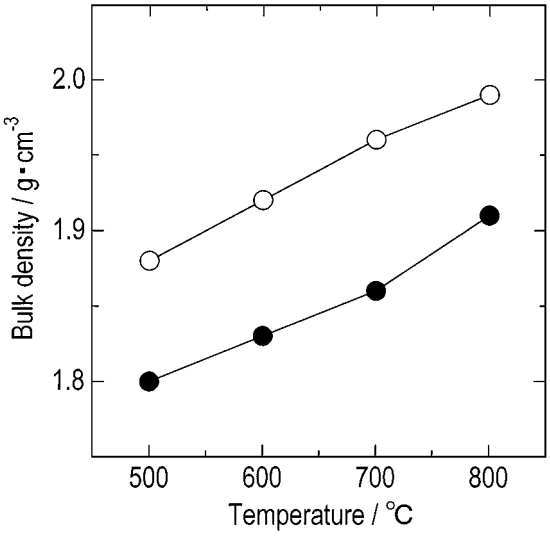

Figure 3 Bulk density plotted against firing temperature for the sintered bodies of alumina-pillared fluorine mica having different particle sizes. ●: sintered body obtained from coarse particles, ○: sintered body obtained from fine particles.

bulk density than those obtained from coarse particles. The weight loss (mass %) during firing, which is ascribable to the dehydration of interlayer water molecules and the dehydroxylation of interlayer polyhydroxoaluminum ions, was almost constant in the firing temperature range of 500–700 °C. On the other hand, the weight loss increased above 800 °C due to the thermal decomposition of the host fluorine mica crystals.

The bulk density of sintered bodies increased almost linearly with increasing firing temperature although the pressed bodies shrank abruptly above 600 °C as shown in Fig. 2. Bulk density depends on the particle size distribution, forming pressure and firing temperature. Reproducibility of green bodies was also somewhat poor because they sometimes had the slightly inclined disk plane with respect to the other plane. This resulted in the increase of the standard deviations for the shrinkage perpendicular to the disk plane. Furthermore, bulk density is related not only to the shrinkage perpendicular to the disk plane but also the shrinkage parallel to the disk plane. The latter shrinkage considerably contributes to bulk density even though its shrinkage is small. In addition, bulk density also depends on the sample weights. The accumulated effects of these factors explain that the change of density don't necessarily reflect the deviated plots of the perpendicular shrinkage from the linear relation.

Fig. 4 shows the XRD patterns of alumina-pillared fluorine micas fired at different temperatures. The (0 0 1) profiles of the alumina-pillared fluorine micas obtained from fine particles become weakened and broadened, compared with those obtained from coarse particles. In addition, the sintered products obtained from fine particles gave weaker and broader lines of high-order (0 0 l) reflections. These facts indicate that the sintered products obtained from fine particles have thinner c^*-dimension of coherent layer stacking sequences, i.e., lower crystallinity. When firing temperature was above 800 °C, the pillared structures collapsed despite of the particle sizes of host mica crystals. The

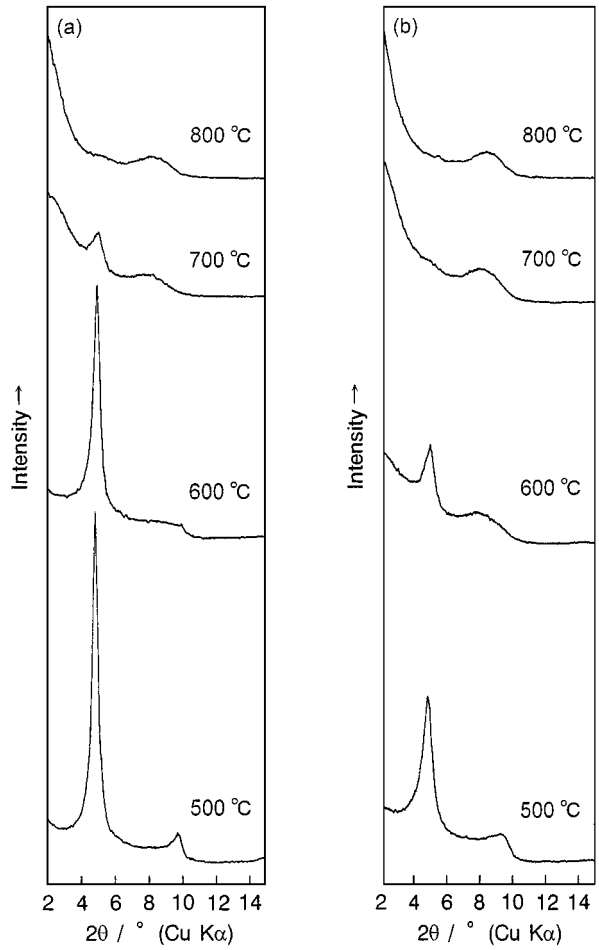

Figure 4 X-ray diffraction patterns for the sintered bodies of alumina-pillared fluorine micas fired at different temperatures. (a) sintered body obtained from coarse particles, (b) sintered body obtained from fine particles.

sintered bodies obtained from coarse particles retained the (0 0 1) reflection of 1.8 nm phase [2θ: 5° (CuK_α)] at 700 °C while those obtained from fine particles lost their long basal spacings. This indicates that thermal durability of the pillared mica structure depends on the particle size of host crystals and that thermal durability of sintered bodies can be improved by using coarse particles. It is also clear that the sintered bodies of alumina-pillared fluorine micas can be prepared by firing at relatively lower temperatures without adding binders.

Fig. 5 shows SEM photographs of the fracture surface for the sintered bodies obtained at 600 °C. The direction of the pressing axis is shown by the arrow. The microstructure of the sintered bodies consists of the interlocking flakes of pillared micas which are curled or corrugated. However, they are loosely oriented vertically toward the direction of the pressing axis on molding, as described previously. Well-developed cleavage lines are sometimes observed on the alumina-pillared mica crystals.

Al contents for the alumina pillared-fluorine micas obtained from coarse particles and fine particles were 2.11 (0.05) and 2.72 (0.06) mol (Al)/Si_4O_{10}, respectively, where the standard deviations are shown in the parentheses. The larger Al content for the pillared micas obtained from fine particles probably results from

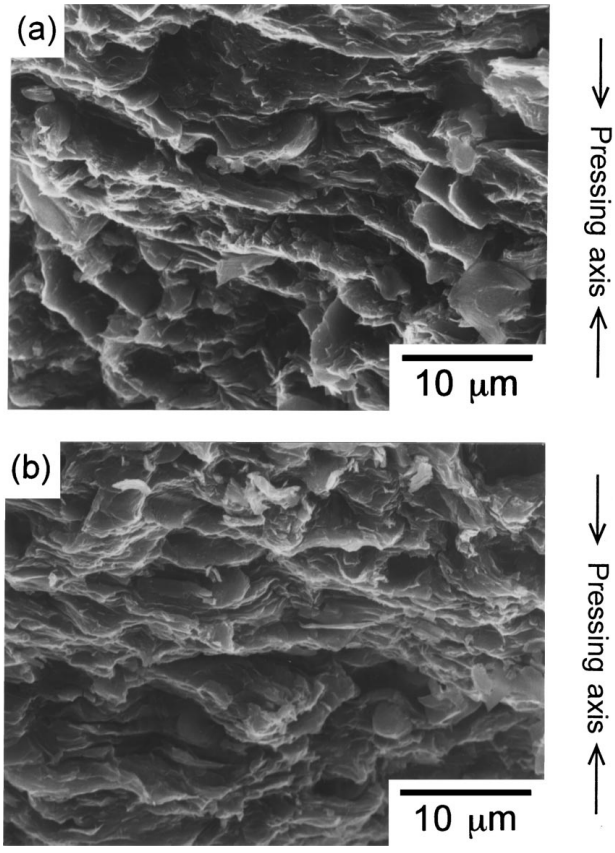

Figure 5 SEM photographs of the fracture surface for the sintered bodies of alumina-pillared fluorine micas fired at 600 °C. (a) sintered body obtained from coarse particles, (b) sintered body obtained from fine particles.

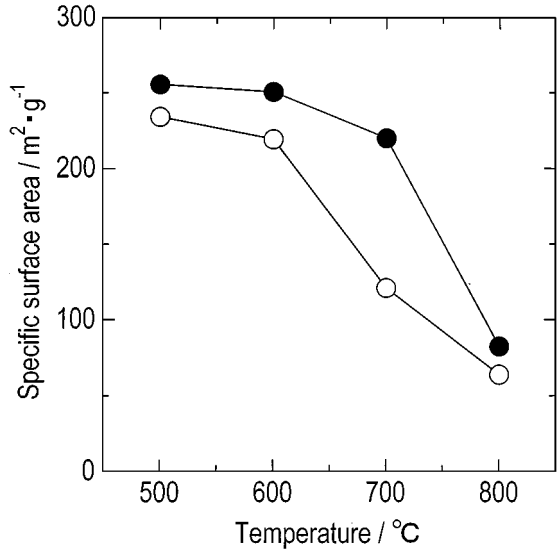

Figure 6 Relation between specific surface area (BET) and firing temperature for the sintered bodies of alumina-pillared fluorine micas. ●: sintered body obtained from coarse particles, ○: sintered body obtained from fine particles.

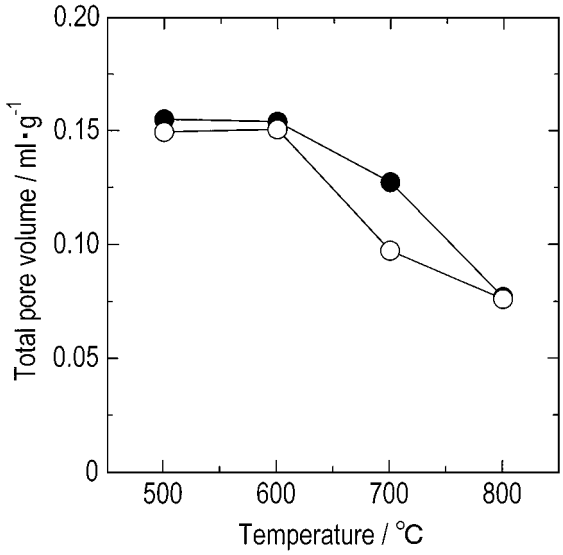

Figure 7 Relation between total pore volume and firing temperature for the sintered bodies of alumina-pillared fluorine micas.●: sintered body obtained from coarse particles, ○: sintered body obtained from fine particles.

the contribution of higher cation exchange ratio of the interlayer cations and the adsorption of polyhydroxoaluminum cations onto the outer surface of host mica crystals. Gels prepared from polyhydroxoaluminum solution provide activated alumina upon heating above 500 °C [11]. Thus, polyhydroxoaluminum cation adsorbed on the outer surfaces and edges may be contributory to sintering upon heating.

In the previous study of complex formations using Na-taeniolite series fluorine micas [$Na_xMg_{3-x}Li_xSi_4O_{10}F_2$; $x \geq 0.6$] [3], pillared micas having ideal stacking sequences were formed only when host crystals were transformed into Li^+-exchanged forms before the intercalation process with polyhydroxoaluminum cations. However, Na-TSM used in the present study can intercalate polyhydroxoaluminum cations without the transforming process into Li^+-exchanged forms. This difference of reactivity is ascribable to the difference in swelling characteristics because Na-TSM exhibits free swelling while Na-taeniolite shows limited swelling up to the double layer hydrated state. This also shows that expandability of host crystals is a critical parameter to intercalation of highly polymerized hydoroxocations.

Fig. 6 shows the relationship between specific surface area and firing temperature for the sintered bodies of alumina-pillared fluorine micas having different particle sizes. The sintered bodies obtained from coarse particles have larger specific surface area than those obtained from fine particles. The sintered bodies obtained from coarse particles had a specific surface area of ca. 220 m^2 g^{-1} even after fired at 700 °C. On the other hand, the specific surface area of the sintered bodies obtained from fine particles decreased drastically at 700 °C. These results correspond to the changes in XRD patterns as shown in Fig. 4.

Fig. 7 shows the relationship between total pore volume (<100 nm) and firing temperature for the sintered bodies of alumina-pillared fluorine micas having different particle sizes. The samples are the same as in Fig. 6. The total pore volume for the sintered bodies obtained from coarse particles was larger than that obtained from fine particles. The sintered bodies obtained from coarse particles had larger total pore volume even after sintered at 700 °C, but the total pore volumes of the sintered bodies became almost the same at 800 °C

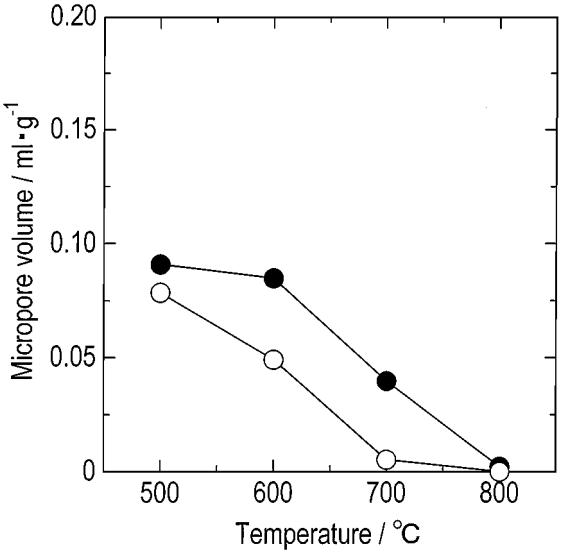

Figure 8 Micropore volume plotted against firing temperature for the sintered bodies of alumina-pillared fluorine micas. ●: sintered body obtained from coarse particles, ○: sintered body obtained from fine particles.

despite of particle sizes. These results probably reflect thermal durability of micropores discussed later.

Fig. 8 shows micropore volume plotted against firing temperature for sintered alumina-pillared fluorine micas. The micropore volume was estimated by the *t*-analysis [12]. The pillared micas obtained from coarse particles had larger micropore volume at all the firing temperatures under the present experimental conditions. The smaller micropore volume of the pillared micas obtained from fine particles probably results from higher Al content since the high Al content leads to the closer packing of alumina pillars in the interlayer region. The micropore volume for each sample decreased considerably at 700 °C. The micropores vanished above 700 °C for the pillared micas obtained from fine particles and above 800 °C for those obtained from coarse particles, respectively. The vanishment corresponds to the collapsion of the pillared structure; the dependence of microporous characters on the particle size disappears when the pillared structure is collapsed.

The pore size distribution curves of alumina-pillared fluorine micas sintered at different temperatures are shown in Fig. 9. All samples gave a sharp peak corresponding to a pore diameter around 4 nm. The pores around 4 nm are ascribable to so-called slit pores which originate from the interstratified structure of pillared micas. This sort of pores has also been found in chromia-[4], titania-[5] and alumina-pillared fluorine micas [3]. The peak of slit pores shifts gradually to smaller diameter sides with increasing firing temperature. A shoulder which appears at the smaller diameter sides below 3 nm becomes weaker with increasing firing temperature, indicating gradual collapsing of the interstratified structure of pillared micas. The shoulder below 3 nm for the pillared micas obtained from coarse particles was stronger than that obtained from fine particles, indicating the higher micropore volume. The difference in the intensity of the shoulder between the two-series samples probably reflects the difference in the pillar density described above.

These results indicate that thermal stability of alumina-pillared fluorine micas obtained from coarse particles is higher than that obtained from fine particles and that the microporous characters depend on the particle size of host mica crystals, especially on the c^*-dimension of host mica crystals.

The sintered bodies were found to be well machinable. The example of the drilled specimen is shown

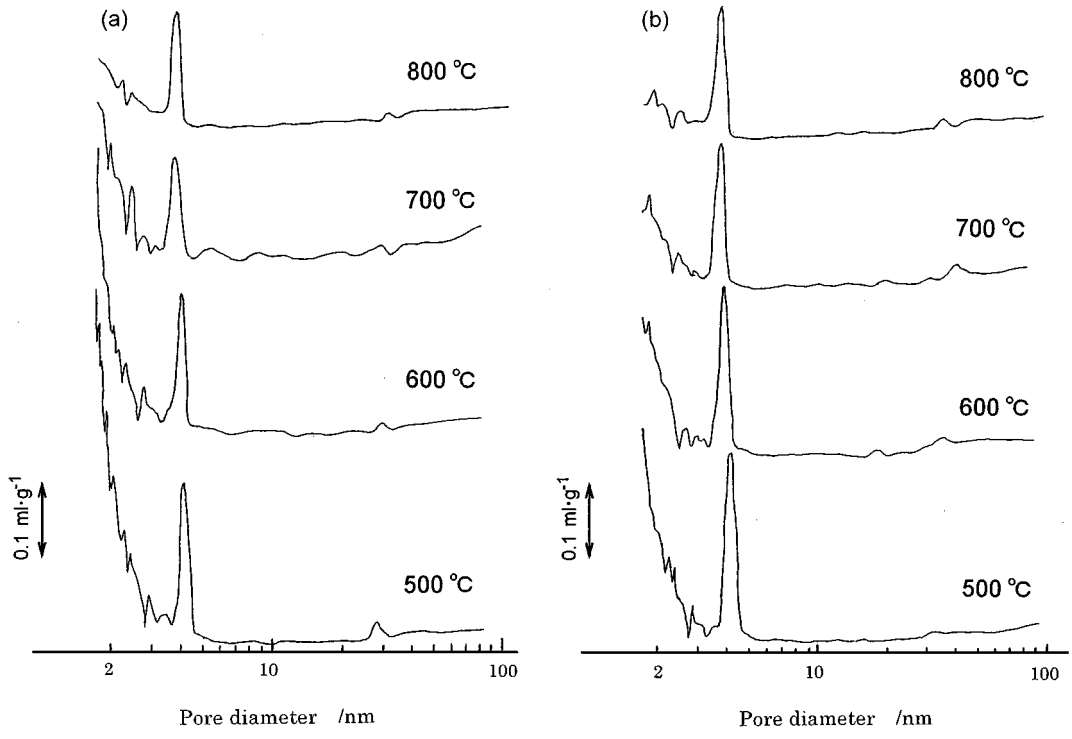

Figure 9 Pore size distribution curves for the sintered bodies of alumina-pillared fluorine micas fired at different temperatures. (a) sintered body obtained from coarse particles, (b) sintered body obtained from fine particles.

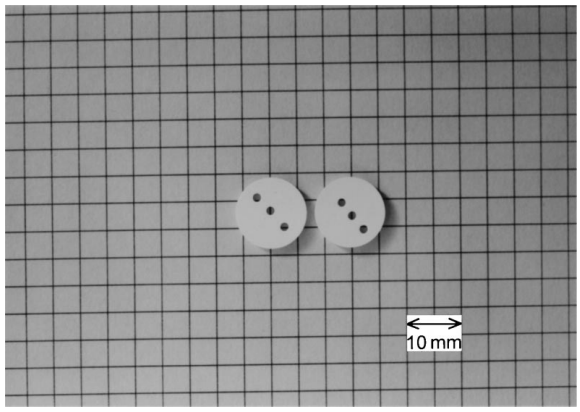

Figure 10 Photograph showing machinability of the sintered body of the alumina-pillared fluorine mica (coarse particles).

in Fig. 10. The good machinability should result from the house-of-cards like microstructure [13] of the interlocking flakes of cleavable mica crystals. Fired bodies retained their shapes even when they were immersed in boiling water for 4 h and showed the bending strength of ca. 20 MPa. The strength is not high but sufficient to handle without dusting under conventional conditions.

4. Conclusion

Powder compacts of alumina pillared fluorine micas having different particle sizes were fired to obtain sintered bodies having microporous characters. Effects of particle size on thermal durability and microporous characters of sintered bodies were investigated. The results are summarized as follows:

1. Sintered bodies of alumina-pillared fluorine micas were obtained by firing the powder compacts of alumina pillared fluorine micas at 500–800 °C. The pillared structure of the sintered products remained in the firing temperature range of 500–700 °C, but collapsed above 800 °C.

2. Microporous characters of the sintered bodies depend on the particle size of host mica crystals. The sintered bodies obtained from coarse particles had larger specific surface area and micropore volume than those obtained from fine particles.

3. Thermal durability of the pillared structure depends on the particle size of alumina-pillared fluorine micas, especially on the c^*-dimension of the host mica crystals; the sintered bodies using coarse particles exhibited better thermal stability.

4. The sintered bodies were found to be machinable. The machinability is ascribable to the interlocking microstructure of flaky cleavable mica crystals. Sinterability without adding extra binders should enable the pillared fluorine micas to use as not only powders but also sintered bodies.

References

1. K. KITAJIMA and N. DAIMON, *Nippon Kagaku Kaishi*, (1975) 1123.
2. K. KITAJIMA, F. KOYAMA and N. TAKUSAGAWA, *Bull. Chem. Soc. Jpn.* **58** (1985) 1325.
3. T. FUJITA, K. KITAJIMA, S. TARUTA and N. TAKUSAGAWA, *Nippon Kagaku Kaishi* (1993) 1123.
4. T. YAMAGUCHI, S. MATSUKURA, T. FUJITA, N. TAKUSAGAWA and K. KITAJIMA, *ibid.* (1997) 862.
5. K. KITAJIMA and F. KUNIYOSHI, *Solid State Ionics* **101–103** (1997) 1099.
6. T. YAMAGUCHI and K. KITAJIMA, *J. Mater. Sci.* **33** (1998) 653.
7. Y. MORIKAWA, K. TAKAGI, Y. MORO-OKA and T. IKAWA, *J. Chem. Soc., Chem. Commun.* (1983) 845.
8. R. E. MESMER and C. F. BAES, JR. *Inorg. Chem.* **10** (1971) 2290.
9. J. W. AKITT and A. FARTHING, *J. Chem. Soc., Dalton Trans.* (1981) 1624.
10. T. FUJITA, K. KITAJIMA, S. TARUTA and N. TAKUSAGAWA, *Nippon Kagaku Kaishi* (1993) 319.
11. T. FUJITA, T. YAMAGUCHI, N. TAKUSAGAWA and K. KITAJIMA, *J. Ceram. Soc. Japan* **106** (1998) 1017.
12. B. C. LIPPENS and J. H. DE BOER, *J. Catal.* **4** (1965) 319.
13. G. H. BEALL, in "Advances in Nucleation and Crystallization in Glasses" edited by L. L. Hench and S. W. Freiman (American Ceramic Society, 1972) p. 251.

Received 25 November 1998
and accepted 23 June 1999